AD-A124 002 JOURNAL OF NANJING INSTITUTE OF TECHNOLOGY (SELECTED ARTICLES)(U) FOREIGN TECHNOLOGY DIV WRIGHT-PATTERSON AFB OH Q HUANG ET AL. 09 DEC 82 FTD-ID(RS)T-0958-82 1/1

UNCLASSIFIED F/G 5/1 NL

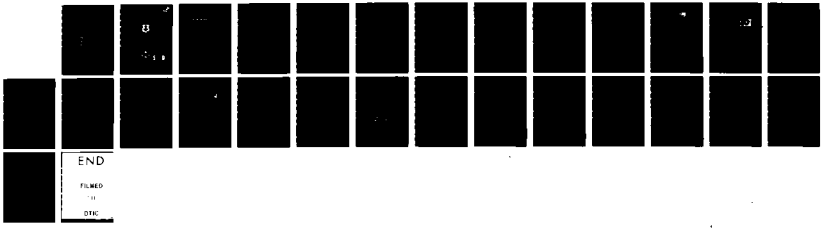

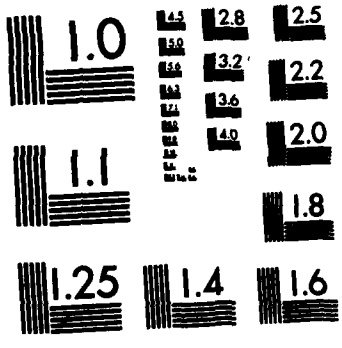

MICROCOPY RESOLUTION TEST CHART
NATIONAL BUREAU OF STANDARDS-1963-A

FTD-ID(RS)T-0958-82

AD A124002

FOREIGN TECHNOLOGY DIVISION

JOURNAL OF NANJING INSTITUTE OF TECHNOLOGY

(Selected Articles)

DTIC FILE COPY

DTIC ELECTE S JAN 3 1 1983 D

D

Approved for public release;
distribution unlimited.

83 01 31 149

EDITED TRANSLATION

FTD-ID(RS)T-0958-82 9 December 1982

MICROFICHE NR: FTD-82-C-001649

JOURNAL OF NANJING INSTITUTE OF TECHNOLOGY
(Selected Articles)

English pages: 23

Source: Nanjing Daxue Xuebao, Nr. 1, 1982,
pp. 102-112

Country of origin: China
Translated by: LEO KANNER ASSOCIATES
F33657-81-D-0264
Requester: FTD/TQTD
Approved for public release; distribution unlimited.

Accession For
NTIS GRA&I [X]
DTIC TAB [ ]
Unannounced [ ]
Justification
By
Distribution/
Availability Codes
Dist | Avail and/or Special
A

THIS TRANSLATION IS A RENDITION OF THE ORIGINAL FOREIGN TEXT WITHOUT ANY ANALYTICAL OR EDITORIAL COMMENT. STATEMENTS OR THEORIES ADVOCATED OR IMPLIED ARE THOSE OF THE SOURCE AND DO NOT NECESSARILY REFLECT THE POSITION OR OPINION OF THE FOREIGN TECHNOLOGY DIVISION.

PREPARED BY:

TRANSLATION DIVISION
FOREIGN TECHNOLOGY DIVISION
WP-AFB, OHIO.

Table of Contents

GRAPHICS DISCLAIMER

All figures, graphics, tables, equations, etc. merged into this translation were extracted from the best quality copy available.

THE SEALED-OFF COPPER CHLORIDE LASER WITH SELF-HEATED DESIGN*

by Huang Qiwen, Zhang Mingbao, Deng Honglin, Zhao Shiming and Yang Zhengming

Abstract

This paper presents the structure of the quartz discharge tube with concave tanks, and its laser operating characteristics are studied. The results obtained were an average output power of 0.7 watts, a volume energy density of 1.46$\mu J/cm^3$, an overall efficiency of 0.16% and a continuous operation of 170 hours.

Preface

The efficiency of existing gas lasers has been disappointing. Aside from the infrared carbon dioxide laser, their overall efficiency is lower than 0.1%. In 1966, Walter [1] first discovered a pulsed laser oscillation with copper atoms of 5106Å ($4^2P_{3/2}$-$4S^2D_{5/2}$) and 5782Å ($4^2P_{1/2}$-$4S^2D_{3/2}$). This device uses pure copper as the working substance and operates under a temperature higher than 1500°C. As a result, the apparatus is complex and expensive.

After 1973, C.S. Liu [2] and C.J. Chen [3] et al followed by using copper halide as the working substance. Under a low temperature of 400-600°C, they discovered the laser emission action of double pulse discharged copper steam. Following this, a repetition pulse pumping technique with a frequency higher than 10 kilocycles was also developed [4] which resulted in a noticeable rise in the average power level of the copper halide laser.

*Received October 24, 1981

However, because the halide system has a cumulative effect under multi-pulse operation, the composite mechanism of the copper atom's quenching and electronegativity gas discharge have complex dynamic processes. During the initial period of the development of this device, it could only operate for several hours and to date it is still in the laboratory stage. In 1978, C.S. Lin et al obtained results of a volume energy ratio of 2 microjoule/centimeter^3, efficiency of 0.2% and total operating time exceeded 100 hours [5]. This is the highest level reached by a sealed-off discharge device with self-heated design.

To carry out practical tests for the sealed-off CuCl laser with self-heated design, we designed a discharge tube structure with concave tanks and radiating shaped molybdenum tube electrodes and used the sealing-in technique of first-order transition DWQ glass. Experimental research was carried out on a CuCl laser with a 1.2 centimeter diameter discharge tube and an activation area length of 38 centimeters. The results obtained were an average laser power of 0.70 watts, a volume energy ratio of 1.46 microjoule/centimeter^3, a total efficiency of 0.16% and continuous operation for 170 hours.

I. Design Considerations for the Long Life Laser

The sealed-off self-heated CuCl laser with repetitive pulses is a device which uses fast speed pulsed excitation with repetition frequency of ten to several tens of kilocycles and a working substance with heat dissipation heating. The key to designing a long life device is how to control the optimal working temperature so as to attain steady steam pressure, not bring about activation medium overheating and fast speed loss, and simultaneously require that the device operate in an optimal excitation state.

The aim of this paper is to design a functional device with

an average power greater than 500 milliwatts and a life time exceeding 100 hours. For this reason, we made the following design considerations:

1. When selecting the measurements of the activation area, we should comprehensively consider the benefits to the diffusion, collision quenching and resonance capture of the sub-steady state copper atoms. At the same time, we must, as much as possible, decrease the effects of radial electrophoresis and axial electrophoresis.

When ground state copper atom N and tube radius R satisfy $NR \geqslant 10^{15}$ centimeters^{-2}, the 3248Å and 3274Å spectral lines can have complete resonance capture [6]. Under these conditions, the effective life times of upper laser energy levels $4^2P_{3/2}$ and $4^2P_{1/2}$ separately increase from 10 millimicroseconds when there is no capture to 615 and 370 millimicroseconds. As a result, this can lower the pumping conditions.

When there is a small opening and low gas pressure, the quenching mechanism of the sub-steady state atoms is mainly the excitation of the discharge tube wall's collision loss [6]. The diffusion rate constant of the copper atoms is determined by the following formula:

$$K_0 = 6D/R^2 \qquad (1)$$

In the formula

$$D = \frac{3\sqrt{\pi T_g k}}{8N\sqrt{2\mu}\pi r_0^2}$$

In the formula, R is the radius of the discharge tube, N is the buffer gas atom density, T_g is the gas temperature, μ is the reduced mass of the colliding particles, r_o is the sum of the

copper atoms and buffer gas atom radius, k is the Boltzmann constant.

When the diameter of the discharge tube is not large ($\leqslant$ 1 centimeters) and there is low pressure buffer gas, the diffusion rate constant is close to being equal to the quenching rate constant but when the diameter is large the volume composite rate enlarges. Therefore, the diameter of the selected discharge tube must be supported by the circulation of the base state copper atoms. It is also necessary to give consideration to resonance radiation capture. We believe that the selection of a discharge tube with a 1-1.2 centimeter diameter is suitable. This has already been proven through experiments.

The ionization potential of the copper atoms in the copper halide laser's laser medium is very low (7.72 ev) and the copper ions shift toward the cathode under the action of the axial electric field. This creates a non-uniform axial distribution of the copper ions and copper atoms which results in non-uniform discharge. The steady state axial distribution of the sum of the copper ions and copper atom density is [7]:

$$n(Z) = n(0)\exp(-\phi Z) \qquad (2)$$

In the formula

$$\phi = 1.05\,\gamma E_i / T_g$$

In these expressions, n(0) is the steady state density in the area of the cathode, Z is the axial distance from the cathode, γ is the degree of ionization, T_g is the gas temperature.

Based on formula (2), we know that the longer the discharge area, the larger the copper atom density difference of the two

terminals of the electrode. This can cause the production of a local low gain area. Therefore, an extreme enlargement of the length of the discharge tube is not advantageous and it must be appropriately selected.

2. Because of the cumulative effects of multi-pulsed excitation, the electron temperature in the region of the discharge tube's axis can reach to over 1,300^{o}C. An increase of the number of fast speed electrons can cause the system to deviate from the optimal conditions. When the repetition frequency with excitation pulses is increased, this often brings about activation medium overheating which causes the cuprous chloride steam pressure to have a high bias and the activation medium to be exhausted too quickly. For this reason, we must regulate the distance between the working substance and the discharge tube's axis so as to guarantee the optimal steam pressure in order to not bring about working substance overheating.

3. Plasma contraction can occur under a repetition pulsed excitation state causing the volume of the activation area to noticeably shrink and produce unsteady discharge. This is especially serious when there is very high steam pressure. Thus, structurally, the stress should have uniform temperature in the entire activation area and not allow local overheating.

II. Experiment Technique

1. The Laser

Based on the above considerations, we designed a tube body structure with concave tanks as shown in fig. (1).

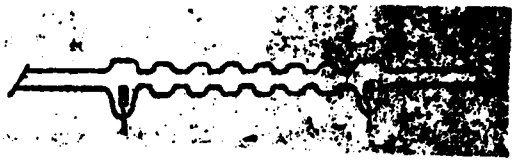

Fig. 1 Schematic of Laser

Tube body measurements: diameter of the discharge tube is 10 millimeters, length of activation area is 380 millimeters, tank depth is 9 millimeters, tank length is 40 millimeters and the distance between the tanks (6 tanks) is 20 millimeters.

Electrode: use of a heat dispersion molybdenum tube electrode with a ϕ13 x 17 millimeter measurement. The electrode lead is sealed by first order transition DWQ glass.

Resonant cavity: cavity length is 1.5 meters, total reflective mirror (hand film) curvature radius is 3 meters and the reflectivity for 5106Å and 5782Å are 99% and 45%. The output mirror is a K_8 glass level mirror which has an unplated film and transmissivity of 5106Å is 88%.

Working substance: cuprous argonide, analytically pure. Before placing it in the storage tank, first preprocess in a vacuum for a long time under a strictly controlled suitable temperature, remove the harmful vapor but do not cause oxidation. Each tube has 17 grams of material distributed into six tanks. The buffer gas is neon and the pressure strength is 20-30 torr.

2. The Excitation Source

We used a resonant charging Bululin* circuit as shown in fig. (2a).

*Bululin should read Blumlein

The entire circuit is composed of three poles: the forward position contact, the buffer amplification (fig. 2b) and the Bululin circuit.

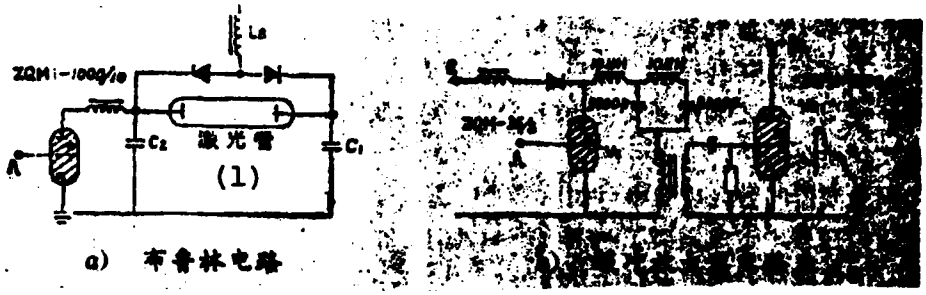

Fig. 2

Key: a) Bululin circuit
b) Buffer amplifier circuit
1) Laser

The forward position contact pulsed generator: frequency is tunable in the 5-30 KC range and there is transformer coupling output.

Buffer amplifier: uses a ZQM-35/3 hydrogen thyratron as this level's switch component. The artificial line has two levels, the inductance is 10 microhenry and the capacitance is 5,000 Pf. The pulse width is 1 microsecond and characteristic impedance is 40 ohm.

The Bululin circuit: in order to create a matching state as much as possible, the stored energy capacitance and charging inductance can both be tuned. The tuning range of the charging inductance is 0.2-1 henry. Actually, L_B=0.2 henry was used as the optimum.

The electric current pulsed waveform is measured by the Rogowski coil and the resistance voltage dividing method. The measured current pulse width is 200 millimicroseconds.

III. Test Results and Analysis

Tests on seven laser tubes with three different types of structures showed that tube body structures with single layer concave tanks obtained relatively good results. Anticipated design requirements were obtained. Their major parameters were as follows:

The laser tube's wall temperature was 350-400^{o}C with an optimum of 380^{o}C.

Average laser power: 0.70 watts.

Pulsed laser energy: 0.04 millijoule.

Volume-energy ratio: 1.46 microjoule/centimeter^{3}.

Repetition frequency: 16.2 kilohertz.

Operating life time: 170 hours.

Efficiency: 0.16%.

Tests proved that the temperature effect of the sealed-off copper halide laser with self-heated design was a very important factor and that the operating frequency, input energy and operating life time of the laser were all restricted by the temperature. If we use a discharge heating working substance and attain steady steam pressure we can expect to have optimum excitation energy for the activation medium. This is without a doubt difficult to do. To investigate the device's temperature effects, we carried out related tests:

1. The Relationship Between the Tube's Wall Temperature and the Output Power

Fig. 3 draws the changes of the laser power following the tube's wall temperature.

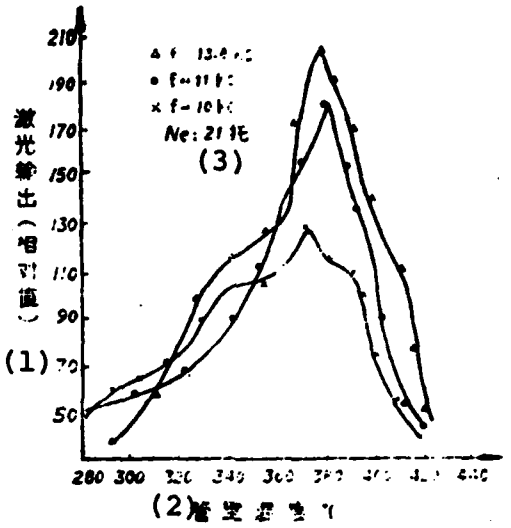

Fig. 3 Changes of the Laser Output Following the Temperature Rises Under Different Frequencies

Key: 1. Laser output (relative value)
2. Tube's wall temperature °C
3. Torr

We know from the curves in the figure that when there is optimum laser output the tube's wall temperature is 340-380°C and after exceeding the optimum temperature the laser power noticeably drops. When this test tube is in a power load of 15.8 watts/centimeter, calculating by the heat conduction of quartz, the inner wall temperature of the discharge tube is about 40°C higher than that of outer wall. That is, the inner wall temperature corresponds to 410-420°C. Because the working substance in the storage tanks is heated by the tube wall, it is only necessary to control the tube's wall temperature in order to be able to control the heating temperature of the working substance.

When the temperature is too high, we can observe the following phenomena:

(1) Cuprous chloride liquid substance boiling and sputtering

causes transmittancy loss of the activation medium for the laser. At the same time, these cuprous chloride particles can also absorb the shift of the electrons backwards toward the cathode. One portion of the particles is deposited in the anode terminal and one portion rushes passed the anode toward the window terminal. This combines into a large particle ball and floats on the Brewster window causing transmittancy loss for the window.

(2) The electric arc contraction increases in strength and the discharge is not steady. When non-uniformity appears in temperature, electric arc bending can appear and the output power begins to fluctuate and even drastically decline.

(3) When we increase the input energy, the laser output power does not increase but even decreases.

To sum up, it can be seen that the way in which we control the operating temperature during the laser operating process is an important factor for prolonging the life of this device.

2. When we use as yet unprocessed or processed but dampened CuCl for the working substance discharge, the negative glow assumes a light blue color and the positive column area assumes a bluish purple color. Even if we change the buffer gas many times, it cannot be completely eliminated. This explains that the existence of working substance vapor is totally harmful. After repeated tests, when vacuum preprocessing was carried out on the CuCl powder for a long time under a strictly controlled suitable temperature, very good results were attained. The processing temperature was the key and when not handled correctly this was harmful and not beneficial.

3. The Rogowski coil was used to measure the discharge electric current waveform as shown in fig. 4.

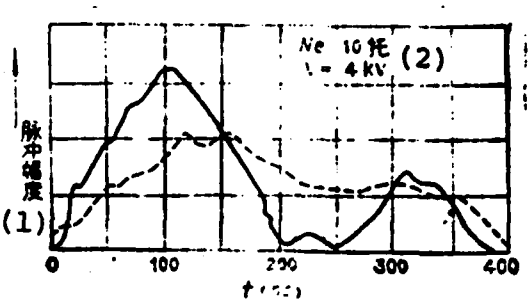

Fig. 4 The Discharge Electric Current Waveform

Key: 1. Pulse amplitude
2. Torr

The width and amplitude of the electric current pulse change with the changes of the discharge tube's temperature. When the tube's wall temperature is relatively low, the cuprous chloride steam pressure is relatively low. The electric current pulse's waveform is indicated by the broken line in the figure. The pulse's effective radius width is 300 millimicroseconds. After the temperature rises, the discharge noticeably contracts, the pulse's leading edge changes suddenly and the amplitude enlarges. The pulse's effective radius width decreases to 100 millimicroseconds.

The electric current waveform in the pure copper laser does not change with the operating temperature. In the copper halide laser, it is possibly related to the action of the halide molecules capturing free electrons and forming negative ions. It is closely related to the temperature.

4. Life Time Tests

Fig. 5 shows the power change of the laser during operation.

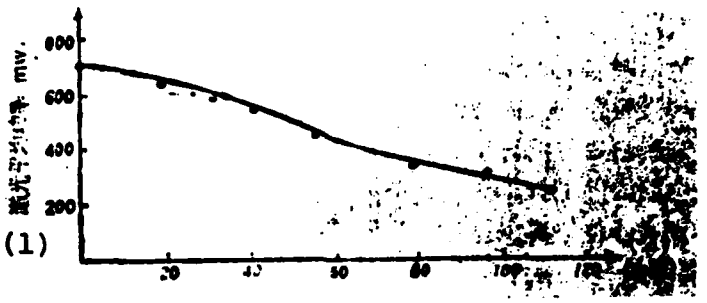

Fig. 5 Laser Power Changes With the Time

Key: 1. Laser's average power (mv)
2. (Hours)

Test conditions: $C_1=C_2=1250Pf$; voltage: V=4.4KV, T-380^{o}C, f=16.2KC.

We can observe the Brewster window polluted by the CuCl during the long life test. The pollution comes from two areas: one is the diffused halide condenses on the window because the window is located in the cold terminal; second, the axial electrophoresis and produced negative electric particles cause the halide to be deposited on the window. We are carrying out further tests to eliminate this type of pollution.

IV. Conclusion

1. The temperature effect of the repetition pulsed cuprous chloride laser with self-heated design is an important factor which influences the life time of the device. Use of a tube structure with concave tanks is advantageous for controlling the tube's wall temperature. It also causes the activation area to maintain uniform steam pressure.

2. When the temperature of the activation area is not uniform, electric arc bending and unsteady discharge can occur. This causes the output power to noticeably decline.

3. The optimum tube wall temperature of this device is 370-380^{o}C.

4. Before using cuprous chloride, we should carry out pre-processing in a vacuum for a long time in a suitable temperature. The vapor which is completely harmful and the impure gas should be eliminated.

References

[1] W.T. Walter, IEEE J. Q. E. Vol. QE-2, P.474. Sept. 1966.

[2] C.S. Liu, Appl. Phys. Lett Vol. 23, P. 92-93, 1973.

[3] C.J. Chen, Appl. Phys. Lett Vol. 23, P. 514-515, 1973.

[4] C.J. Chen, and G.R. Russell. Appl. Phys. Lett Vol. 26, P. 504-505, 1975.

[5] D.W. Feldman, C.S. Liu AD-A053237/46 A.

[6] V. M. Bateni, Quantum Electronics, 7, No. 8, P1813-1820, 1980.

[7] C.S. Liu, J. A. P. Vol. 48, P 194, 1977.

USE OF ELLIPSOMETRY TO MEASURE THE THICKNESS OF LESS THAN 50 Å ULTRATHIN OXIDE FILM ON SILICON*

by Zhang Jiawei and Zhao Zhengping

Abstract

This paper presents a method of using ellipsometry to measure the thicknesses of ultrathin oxide film on silicon. The compositions of 8 Å to 38 Å oxide films has been studied by AES and their refracting power is established. The ellipsometrical parameters corresponding to 0 to 50 Å oxide films have been calculated by computer. At present, the thinnest thickness of oxide film on silicon measured by this method is 6 Å and good reproducibility has been attained.

I. Preface

One key technique in making a solar energy cell with an MIS (metal - insulator - semiconductor) structure is the preparation on the substrate of an ultrathin oxide film with uniform thickness in the 10 Å to 20 Å range.

The capabilities of the non-volatile storage with an MNOS (metal - nitride - oxide - semiconductor) structure is related to the thickness of the ultrathin oxide film. The thicknesses of gate oxide films with extra large scale circuits are being made thinner and thinner. These require instruments and techniques which are convenient, precise and non-destructive and that can

---

Received October 29, 1981.

measure dielectric film thickness lower than several angstrom.

At present, ellipsometry is internationally recognized as the most sensitive instrument for measuring thickness [1]. However, because of the domestic insufficiency of reports on measuring thicknesses less than 100 Å, people have been doubtful as to whether accurate measurements of the thicknesses of ultrathin dielectrics can be made for it. Because we developed the requirements of the MIS solar energy cell and carried out research on how to use ellipsometry to measure the thicknesses of ultrathin oxide film on silicon, we obtained preliminary results. The thinnest thickness of oxide film measured was 6 Å and reproducibility was good. Moreover, it has already been applied in manufacturing devices.

II. The Basic Principles of Measuring Thickness With Ellipsometry

The basic optical path of ellipsometry is shown in fig. 1.

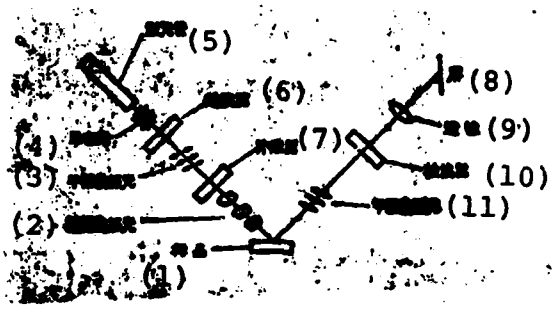

Fig. 1

Key: 1. Specimen
2. Elliptically polarized light
3. Plane polarized light
4. Monochromatic light
5. Laser tube
6. Polarizer
7. Compensator
8. Screen
9. Lens
10. Analyser
11. Plane polarized light

The monochromatic light emitted from the nitrogen-neon laser tube passes the polarizer and becomes plane polarized light. This polarized light is decomposed by a 1/4 wavelength compensator into perpendicular P and S waves. This becomes elliptically polarized light. This elliptically polarized light is reflected many times passed the specimen's surface and the polarization state of the light changes. It generally changes into another type of elliptically polarized light. If the polarizer rotates at this time, it can cause the phase difference of the P and S waves on a certain azimuthal angle to be zero and become plane polarized light. This type of analyzer adjustment causes the light intensity to change and in a certain azimuthal angle of the analyser the light of the analyser output is caused to be weakest. This is equivalent to reaching extinction.

The physical model of the measured ultrathin dielectric is shown in fig. 2.

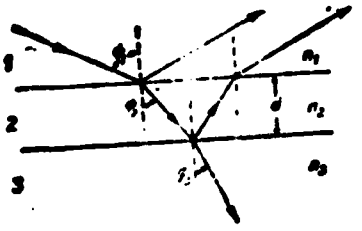

Fig. 2

In the figure, ϕ_1 is the angle of incidence which is fixed at 70°. 1 is the air, 2 is the measured dielectric and 3 is the silicon substrate. The standard equation for the elliptical measurement of the physical model of this type of double layer structure is:

$$\tan\psi e^{i\Delta} = \frac{r_{12}^p + r_{23}^p e^{-i2\beta}}{1 + r_{12}^p r_{23}^p e^{-i2\beta}} \cdot \frac{1 + r_{12}^s r_{23}^s e^{-i2\beta}}{r_{12}^s + r_{23}^s e^{-i2\beta}} \qquad (1)$$

In the equation, r_{12} and r_{23} are the Fresnal reflection coefficients of the 1,2 interface and 2,3 interface which are determined by the following relations.

$$r_{12p} = \frac{n_2 \cos\phi_1 - n_1 \cos\phi_2}{n_2 \cos\phi_1 + n_1 \cos\phi_2}$$

$$r_{12s} = \frac{n_1 \cos\phi_1 - n_2 \cos\phi_2}{n_1 \cos\phi_1 + n_2 \cos\phi_2}$$

$$r_{23p} = \frac{n_3 \cos\phi_2 - n_2 \cos\phi_3}{n_3 \cos\phi_2 + n_2 \cos\phi_3}$$

$$r_{23s} = \frac{n_2 \cos\phi_2 - n_3 \cos\phi_3}{n_2 \cos\phi_2 + n_3 \cos\phi_3}$$

The 2δ in equation (1) is the phase difference caused by the light path difference between the two adjacent reflecting rays. δ and film thickness d have the following relation

$$\beta = \left(\frac{2\pi}{\lambda}\right) d (n_2^2 - n_1^2 \sin^2\phi_1)^{1/2} \qquad (2)$$

In the equation, λ is the wavelength of the helium-neon laser which is equal to 6328 Å. n_1, n_2 and n_3 are the refracting power of the air, dielectric and substrate.

Based on the azimuthal angles of thepolarizer and analyser when there is extinction, after calculations we can obtain Δ and Ψ. We can solve δ with equation (1) and based on the relation of equation (2) we can obtain film thickness d.

Because the solution of equation (1) is relatively complex, the corresponding relational curves of Ψ, Δ and n_2,d calculated by the computer with one machine part automation research were drawn into a chart. The general form is shown in fig. 3.

Each curve corresponds to the refraction index of a specific medium and when the film thickness is zero. Δ is approximately 179.2°. The Δ of an ultra-thin medium will be slightly less than 179°. The method for measuring film thickness using an elliptical polariscope is done by measuring Ψ and Δ at

extinction and then by checking n_2 and d for the intersection points in the figure. (In Fig. 3 the corresponding curves have not been drawn for every film thickness).

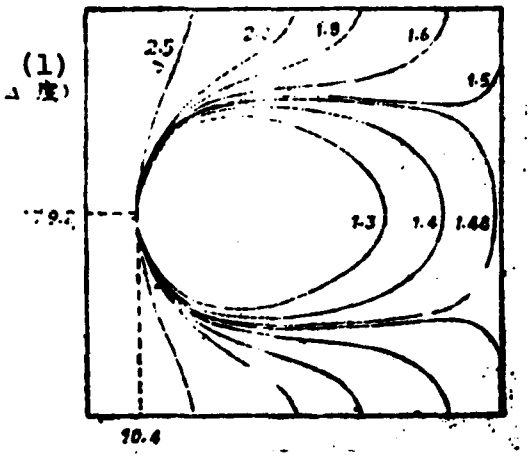

Fig. 3

Key: 1. (Degrees)

III. Measurement of the Thicknesses of Ultrathin Oxide Film

1. Existing Problems

To measure the thicknesses of films less than 100 Å, aside from the sensitivity of the instrument, there are several other problems which must be solved. Firstly, in most situations, elliptical parameters Ψ and Δ are related to the thickness and refracting power of the dielectric (this is based on the fact that ellipsometry can be used to simultaneously measure the film's thickness and refracting power) and the same Δ value corresponds to different thicknesses for different n_2. Yet, when the oxide film is thinner than 100 Å, we can see from fig. 3 that the equal refracting power curves all coincide and in reality there is no way to determine the δ value. Secondly, when the oxide film is very thin, the actually measured Ψ value is often greater than the theoretical value so that the obtained Ψ, Δ point of intersection is outside the above mentioned theoretical curve. Thirdly, the data in the figure expresses the Ψ, Δ data of the corresponding thick film which uses a step length of 20 Å.

Improvements are needed for measuring film thicknesses of several to several tens of angstrom.

2. Solution Methods

We carried out the following work concerning the above mentioned problems.

Based on the report in reference [2], our AES analysis of the thickness of several types of ultrathin oxide film on silicon 8 Å-36 Å as well as the depth distribution of combined argon ion sputtering [3] showed that oxide film with a thickness less than 20 Å is a transition layer between the $Si-SiO_2$. The different thicknesses reflect the different number of layers of the transition layer. Oxide film above 20 Å possesses a more complete SiO_2 layer. Thus, thin oxide film with thickness less than 100 Å should consider the SiO_2 layer and equivalent molecular formula as the transition layer's double layer structure of SiO_2 $(0 < x < 2)$. We determined that the x of ultrathin oxide film with 8 Å, 16 Å, 20 Å and 38 Å is 0.5, 0.7, 1.0 and 1.5. Based on the refracting power and relational curve of x mentioned in reference [4] we can find the corresponding refracting power.

Based on this, we calculated $n_3=3.85-j0.02$ and the Δ, Ψ value corresponding to the various different thicknesses d of n_2 from 1.46 to 2.6. We find that the changes of Ψ under different n_2 were very small and the Δ-D relation was very different. This difference was even greater when the thickness was above 20 Å and the n_2 was between 1.7 and 2.2. When it was hypothesized that this layer of film was completely SiO_2, the measured film thickness tended to be larger than the real film thickness.

The problem of the Ψ deviating from the theoretical value is due to the data coming from the automation research which is hypothetically $n_3=3.85-j0.02$ as well as the silicon wafer being

viewed as the ideal value with no damage. The actual polished piece always has surface damage. Based on the theory of reference [5], the value of Ψ enlarges because of the surface damage. The reason for this is the enlargement of the substrate's refracting power. There was also a difference between the Ψ value measured from the silicon wafer with different techniques of polishing and the theoretical value. This proves that this view is correct. Calculation results showed that the real part of n_3 enlarged from 3.85 to 3.91 and Ψ enlarged 0.4° yet the relational change of d and Δ was not large. This caused us to be able to hypothesize a substrate's refracting power and calculate the thickness based on the change of Δ. Its error is within the accuracy of the instrument.

In view of the above analysis, we hypothesized that the medium's refracting power n_1 is 1.46-2.6 and the substrate's refracting power n_3=3.85-j0.02. Based on equations (1) and (2), we automatically coded a program, used a computer to calculate from 0 to 50 Å and used the Ψ,Δ data corresponding to a step length of 1 Å to resolve the problem of the data processing for measuring the ultrathin dielectric.

3. Test Results

We used a calculated numerical table to carry out a large number of measurements for the natural oxide film thickness of the silicon wafer and ultrathin oxide film thickness of the low temperature growth. The measurement results and growth pattern matched completely. Tables 2 and 3 list the typical results of the residual oxide layer after processing under different techniques. The thicker ones were the original silicon wafer prior to cleaning, those of intermediate thickness were generally the result of semiconductor chemical processing and the thinner ones were the result of special technical processing.

(1)片 号	残留氧化层厚度（Å）(2)	晶 向 (3)
104	32、30、29、30	⟨100⟩
103	19、23、19	⟨100⟩
13	18、19、20	⟨100⟩
15	21、18、19	⟨111⟩
15*	35、36、31	⟨111⟩

Table 1

Key: 1. Wafer number
2. Residual oxide layer thickness (Å)
3. Crystal direction

片 号 (1)	残留氧化层厚度（Å）(2)	晶 向 (3)
301	6，6	⟨100⟩
302	8，9	⟨100⟩
305	9，7	⟨100⟩
306	6，7	⟨111⟩
307	7，8	⟨111⟩

Table 2

Key: 1. Wafer number
2. Residual oxide layer thickness (Å)
3. Crystal direction

Measurement results showed that when multiple measurements of the same point of the same wafer were carried out, reproducibility was good and the error was within $\pm$ 1 Å. There was fluctuation in the thickness of different points of the same

wafer which is a normal phenomenon. The data listed in the above tables are the measurement results of different points of the same wafer.

IV. Verification of the Measured Film Thickness

Because ellipsometry, which was used to measure the thickness, is at present the most sensitive measure, and, as there is no way of using another more accurate method for testing its results, we carried out indirect verification. The aim of this was to appraise the believability of the measurement results.

1. AES Analysis

Besides seeing the ultrathin oxide film with different thicknesses measured by ellipsometry in the depth distribution spectrum corresponding to the different levels of the transition layer, we also carried out component analysis using different energy auger electrons with different escape depths. For example, for a sample with a depth of 23 Å, the O/Si ratio obtained from the silicon LVV transition auger electron information using an escape depth of ~ 4 Å is 1.5 and the O/Si ratio obtained from the KLL transition auger elctron information using an escape depth of ~30 Å is 0.39. We can see from this that a portion of the information obtained at this time comes from the silicon substrate.

2. The electric parameters of the MIS solar cell also provide strong evidence for the film thickness. We used ellipsometry to measure the cell made of a silicon wafer with an oxide film thickness of 12-17 Å. Its open-circuit voltage was greater than 500 mV which proves it is not gold one half contact. Yet at the same time, the density of the short circuit electric current reached 25-28 mA/cm^2 proving that there was very high charge carrier tunneling probability. If the film thickness is not in

this range, then this type of electric parameter cannot be obtained.

3. We also made a sample with a measured film thickness into an MOS capacitor and measured its C-V characteristics. Because of the requirements of the breakdown field intensity, the film SiO_2 cannot be too thin. The ellipsometrical determination was a 47 Å sample. The calculation result of tests using the C-V method was 48 Å. The similar results obtained by using two test methods with completely different principles were very satisfying.

The test instrument which we used was one of several products among the first batch test-manufactured by our institute's machine plant. Before measuring the ultrathin dielectric, we corrected each part of the instrument again so as to guarantee its precision. The entire measurement process was done in a dark room so as to raise observation sensitivity.

We would like to express out thanks to the many comrades in the teaching and research group who carried out a large amount of work.

References

[1] F. Meyer, Sur. Sci. 56,37, 1976.

[2] J. S. Johannessen et al, J. Appl. Phys., Vol. 47,3028, 1976.

[3] This paper was presented at the 1981 All China Annual Meeting of Semiconductor Physics.

[4] S.H. Wemple, Phys. Rev., B7, 3767, 1973.

[5] K. Vedam, Sur. Sci., 56,221, 1976.

[6] K. Vedam et al, Sur. Sci., 29,379, 1972.